

FLUID IMPACT AND SPATIAL AND TEMPORAL EVOLUTION OF NORMAL FAULTING IN LIMESTONES. A CASE STUDY IN THE BURDUR-ISPARTA REGION (SW TURKEY)

Griet VERHAERT¹, Philippe MUCHEZ¹, Eddy KEPPENS² & Manuel SINTUBIN¹

(13 figures)

1. *Geodynamics and Geofluids Research Group, Afdeling Geologie, Katholieke Universiteit Leuven, Celestijnenlaan 200E, B-3001 Leuven, Belgium, e-mail: philippe.muchez@geo.kuleuven.be*

2. *Department of Geology, Vrije Universiteit Brussel, B-1050 Brussel, Belgium*

ABSTRACT. The development of normal faults in carbonates in upper-crustal conditions (< 1-3 km) is a very complex process, because of the interaction of mechanical and chemical processes. This paper investigates the effect of the architecture of normal faults on fluid flow at different depths. This study has been performed on a well-exposed normal fault complex, i.e. the Sarikaya fault complex, in the Burdur area, situated ~120 km north of Antalya (SW Turkey). The particular outcrop allowed studying fault zone architecture and fault-related precipitates at different structural levels over a vertical distance of ~250m.

The earliest stage of normal fault zone development occurs with the upward propagation of a neoformed fault. Seismic deformation is responsible for the development of a low permeable stylobreccia at depth. During fault movement, permeability is greatly enhanced at the fault plane contact. This permeability enhancement causes a fluid-pressure differential responsible for co-seismic, focused fluid flow parallel with the fault plane. Calcites on the fault plane and in veins in the damage zone precipitated from rock buffered fluids ($\delta^{13}\text{C} = -0.1$ to $+2.5\text{‰}$ V-PDB, $\delta^{18}\text{O} = -4.0$ to -0.7‰). During repetitive increments of seismic slip, permeability is renewed at the fault plane contact and fluids are expelled. These increments of seismic slip lead to fault propagation. This fault propagation is accompanied by the formation of a fault precursor breccia ahead of the fault tip by intense localized fragmentation and brecciation of the adjacent shatter zone. This leads to a cohesive breccia where confining pressure is still high and an incohesive breccia near the surface. The cohesive damage zone acts as a combined conduit-barrier system and a more dispersed, co-seismic fluid flow is present near the fault plane contact. The near-surface, incohesive damage zone is characterised by a high permeability, which leads to a highly dispersed fluid flow. Meteoric water can easily infiltrate which leads to static fluid interaction with the normal fault.

Later propagation of a fault plane through its fault-precursor breccia belt results in the deformation concentrated along the fault plane and the evolution of the fault-precursor into a fine gouge or attrition breccia. Once a slip plane reaches the free surface by propagating through its own (in)cohesive breccia belt, co-seismic deformation is restricted to a relatively narrow zone of attrition. In the case of the cohesive damage zone, fluid flow is enhanced adjacent to the slip plane. The fault related fluid is in equilibrium.

KEYWORDS: fault permeability, fault zone architecture, fluid flow, normal fault, stable isotopes, SW Turkey

1. Introduction

The development of normal faults in carbonates in upper-crustal conditions (< 1-3 km) is a very complex process, because of the interaction of mechanical and chemical processes (e.g. Sibson, 2000). The aim of this paper is to demonstrate that the fault architecture of the normal faults at different depths has an effect on the behaviour of the fault with regard to fluid flow. Calcites precipitating from these fluids can be used to deduce the origin of the fluids and to reconstruct the palaeofluid flow pattern in a normal fault setting. This determines the fault zone architecture, commonly composed of a damage zone and a fault core, as well as its permeability architecture. Fault zones can indeed act as barriers, conduits, or mixed conduit/barrier systems (Smith *et al.*, 1990; Antonellini & Aydin, 1994;

Billi *et al.*, 2003; Micarelli *et al.*, 2006; Breesch *et al.*, in press). The permeability architecture can, moreover, vary through the evolution of a fault zone (Smith, 1980; Pittman, 1981; Anderson *et al.*, 1994; Evans *et al.*, 1997). Some faults form conduits early in their history (Gibson, 1994; Roberts, 1995; Tellam, 1995), i.e. the “conduit stage”, only to become barriers to fluid flow later in their history, i.e. the “evolved stage” (Billi *et al.*, 2003). Because of the potentially high permeability of normal faults, their importance as channel ways for hydrothermal fluids and as sites favourable for mineral deposition has long been recognized (Hulin, 1929; Newhouse, 1942; Muchez *et al.* 2005). Most authors relate this fluid behaviour to the episodic or cyclic nature of faulting processes (Etheridge *et al.*; 1984; Sibson *et al.*, 1988; Knipe, 1993; Cox *et al.*, 2001).

Crustal deformation processes clearly influence fluid flow. These fluid interactions may be broadly grouped into those that are static and those that are dynamic with episodes of fluid redistribution modulated by fault slip increments coupled to the seismic stress cycle (Sibson, 2000). Static interactions are due to the relative permeability of the fault core, the damage zone of the faults and the country rock. These permeability differences will determine if a fault is transmissive to flow or acts as an impermeable barrier (Caine *et al.*, 1996). As a fault evolves, its structure and hydraulic properties may vary over time and space. Fault zone architecture and related permeability structures form primary controls on fluid flow in upper crustal brittle zones. Evidence for fluid interaction and involvement with normal faults at shallow depths (<1-3 km) is abundant, though the problem stays of determining under what conditions such structures act as fluid barriers or conduits, if fault permeability is due to static or dynamic reasons, and what localises fluid fluxes at particular sites.

The aim of this paper is to demonstrate that the fault architecture of the normal faults at different depths has an effect on the behaviour of the fault with regard to fluid flow. Calcites precipitating from these fluids can be used to deduce the origin of the fluids and to reconstruct the palaeofluid flow pattern in a normal fault setting. Besides these calcite precipitates, also the different constituents of the fault zone, i.e. fault core and damage zone, can be geochemically investigated. Understanding the combined impact of mechanical and chemical changes in each of the two fault zone components is crucial to a better understanding of possible heterogeneity and anisotropy in fault zones.

This study has been performed on a well-exposed normal fault complex, i.e. the Sarıkaya fault complex, in the Burdur area, situated ~120 km north of Antalya (SW Turkey; Fig. 1). The particular outcrop allowed studying fault zone architecture and fault-related precipitates at different structural levels over a vertical distance of ~250m.

2. Geological setting

The Sarıkaya fault complex (SFC) occupies a particular setting (Fig. 1). It is located at the convergence of the WSW-ENE trending Sagalassos fault (SF) (Similox-Tohon *et al.*, 2006) and the SSW-NNE trending Bassaray-Baskoy fault zone (BBFZ) (Similox-Tohon, 2006). These normal faults all belong to the northeastern extremity of the Fethiye-Burdur fault zone (FBFZ). The latter is considered the northeastern on-land continuation of the offshore Pliny-Strabo trench (Barka *et al.*, 1995; Bozkurt 2001). It is the crustal expression of a lithospheric lateral tear fault, caused by the detachment of the subducting African plate underneath the Aegean-Anatolian/Eurasian plate.

Recent and historical earthquakes (Similox-Tohon *et al.*, 2005; Similox-Tohon *et al.*, 2006; Sintubin *et al.*, 2003) evidence that these normal fault systems are still active. Their characteristic geomorphological expression thus allows identifying the active fault systems in the area. The normal fault activity started in Late Miocene – early Pliocene times (~5Ma; Şengör *et al.*, 1985; Bozkurt 2001) and recorded a complex history of a changing stress field (Verhaert *et al.*, 2006). The faults of the SFC bear evidence of Late Miocene to Holocene fault activity.

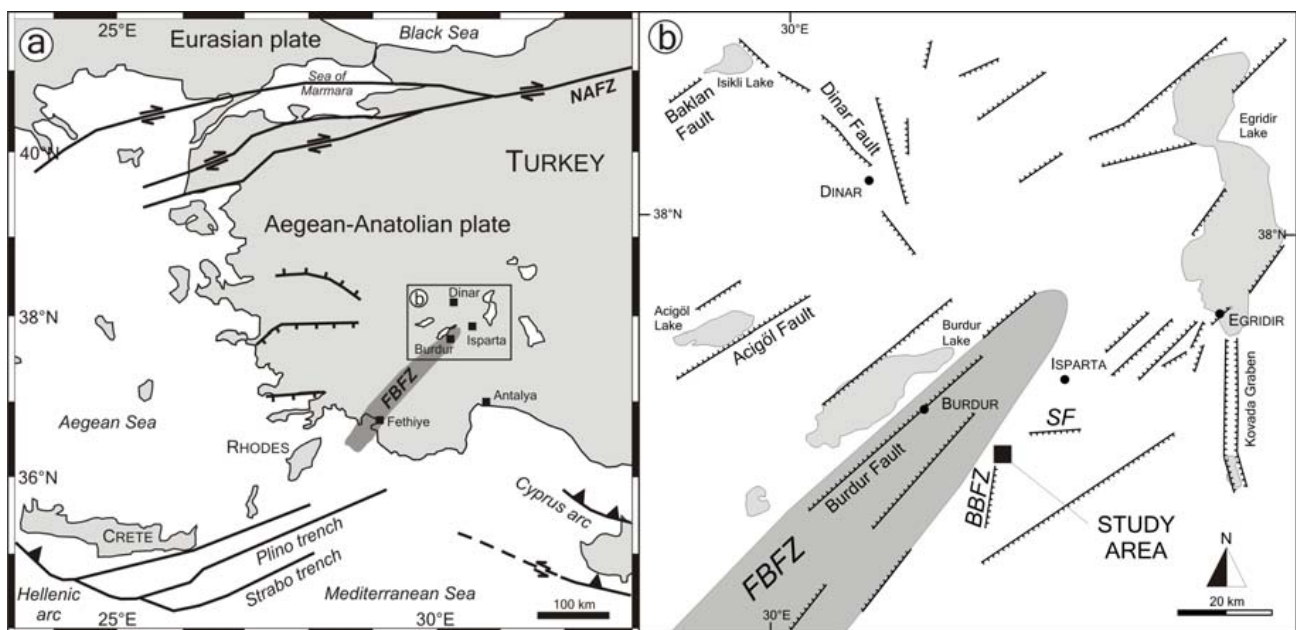


Figure 1. Geodynamic setting of the Burdur-Isparta area. a) Tectonic setting of the Fethiye-Burdur Fault Zone (FBFZ) in SW Turkey (after ten Veen, 2004). NAFZ: North Anatolian Fault Zone. b) Simplified active fault map of the region of the lakes at the northeastern extremity of the Fethiye-Burdur fault zone (FBFZ) (after Similox-Tohon *et al.*, 2008). BBFZ: Bassaray-Baskoy Fault Zone; SF: Sagalassos Fault. The study area of the Sarıkaya fault complex is located at the northern extremity of the BBFZ.

The protolith of the SCF is a middle Triassic to Jurassic, cohesive (low-porosity) bioclastic limestone, belonging to the Lycean nappes (Poisson *et al.*, 1984). The bioclastic limestone is mainly characterised by bioclastic wackestone- to grainstones with crinoids, foraminifers, bivalves, calpionellids, ostracods, gastropods, sponge spicules, rudist fragments, pellets, micritised grains and clasts. The fossils may be micritised. The limestones are often intensely recrystallized and veined and stylolites are abundant (Degryse *et al.*, 2003). The veins are filled with equant to blocky calcites. The isotopic composition of the limestones varies between 1.5 and 3.6‰ VPDB for carbon and between -4.1 and -0.2‰ for oxygen (Muechez *et al.*, 2008 ; Degryse *et al.*, 2008). This range is similar to the marine isotopic composition of Middle Triassic carbonates ($\delta^{18}\text{O} = -2$ to -3‰ VPDB, $\delta^{13}\text{C} = 0$ to $+4\text{‰}$ VPDB; Frisia-Bruni *et al.*, 1989) and of Lower Jurassic carbonates ($\delta^{18}\text{O} = -3.2$ to $+0.7\text{‰}$ VPDB, $\delta^{13}\text{C} = -0.7$ to $+4.3\text{‰}$ VPDB; Rosales *et al.*, 2001). In the study area also an Upper Senonian ophiolitic mélangé and olistostrome unit is cropping out, as well as Quaternary scree and slope deposits.

3. Methodology

The fault rock fabrics were macroscopically and microscopically described. Thin sections were examined by conventional and cathodoluminescence petrography. A Technosyn Cold Cathodo Luminescence Model 8200MKII was operated at 16-20 kV, 400-620 μA gun current, 5 mm beam width and 6.65 Pa vacuum. The multiple coatings in the fault core and the limestones and veins in the damage zone have been analysed for their oxygen and carbon isotopic composition. Samples were taken with a Merchantek® micro mill. A micro mill is a sampling device designed for high resolution milling to recover sample powder for further analysis. Stable isotope analyses of these samples were carried out using a ThermoFinnigan Kiel III carbonate device interfaced with a ThermoFinnigan Delta Plus XL IRMS. All values are reported in per mil (‰) relative to V-PDB (belemnite of the Cretaceous Pee Dee Formation) by assigning a $\delta^{18}\text{O}$ value of -2.20‰ and a $\delta^{13}\text{C}$ value of $+1.95\text{‰}$ to the international reference material, NBS19 (Coplen *et al.*, 1983). Sample repeatability, based on laboratory standard was better than 0.02‰ (1σ) for $\delta^{13}\text{C}$ and 0.04‰ for $\delta^{18}\text{O}$ (1σ).

4. Fault complex analysis

In the SFC, 4 different fault zones have been studied (Fig. 2). They are situated at different elevations between ~1500m and 1700m: Lineament fault zone (LFZ) ~1500m, Quarry fault zone (QFZ) ~1550m, Eastern Summit fault zone (ESFZ) ~1650m and Western Summit fault zone (WSFZ) ~1700m. Two fault zones, the LFZ and the WSFZ, are trending SSW-NNE. The two other fault zones, the ESFZ and the QFZ, are WNW-ESE oriented. Each of the fault zones is characterised by typical fault zone

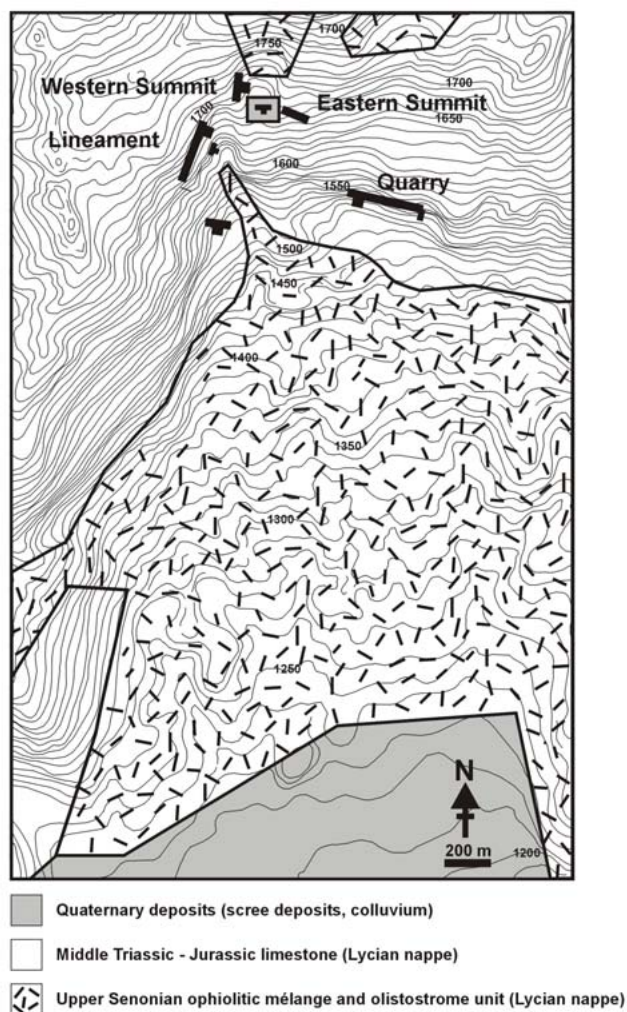


Figure 2. Schematic map (modified after Şenel, 1997 and Verstraeten *et al.*, 2000) with the location of the Sarıkaya Lineament, Sarıkaya Western Summit, Sarıkaya Eastern Summit and Sarıkaya Quarry. Geometry and palaeostress tensor of the fault data in the Sarıkaya area (modified after Verhaert *et al.*, 2006).

architecture, consisting of a damage zone and a fault core. Moreover, individual fault planes are commonly coated with a fault-related calcite precipitate. The Lineament fault zone consists of a major normal fault with an orientation of 190/82 and dip-slip normal movement and 8 nearly parallel normal faults planes that are oriented between 0/90 and 160/70, also with dip-slip movement. The orientation data are given in azimuth convention (right-hand rule), i.e. strike direction/dip. A large fault zone is present at the Western Summit of Sarıkaya (Fig. 2). The fault zone comprises seven quasi parallel slip planes and zone parallel layers of fault breccia. The fault zone shows multiple slip planes with an orientation of 10/80 and is located at a height between 1700 and 1750 m. At Sarıkaya Eastern Summit (Fig. 2), a large undulating fault plane in limestone is present. This undulating fault plane has an orientation of 110/60 and 138/85. On the fault plane, a breccia composed of ophiolitic and limestone fragments are present. This breccia is cemented and covered by a thick flowstone. The Sarıkaya Quarry fault

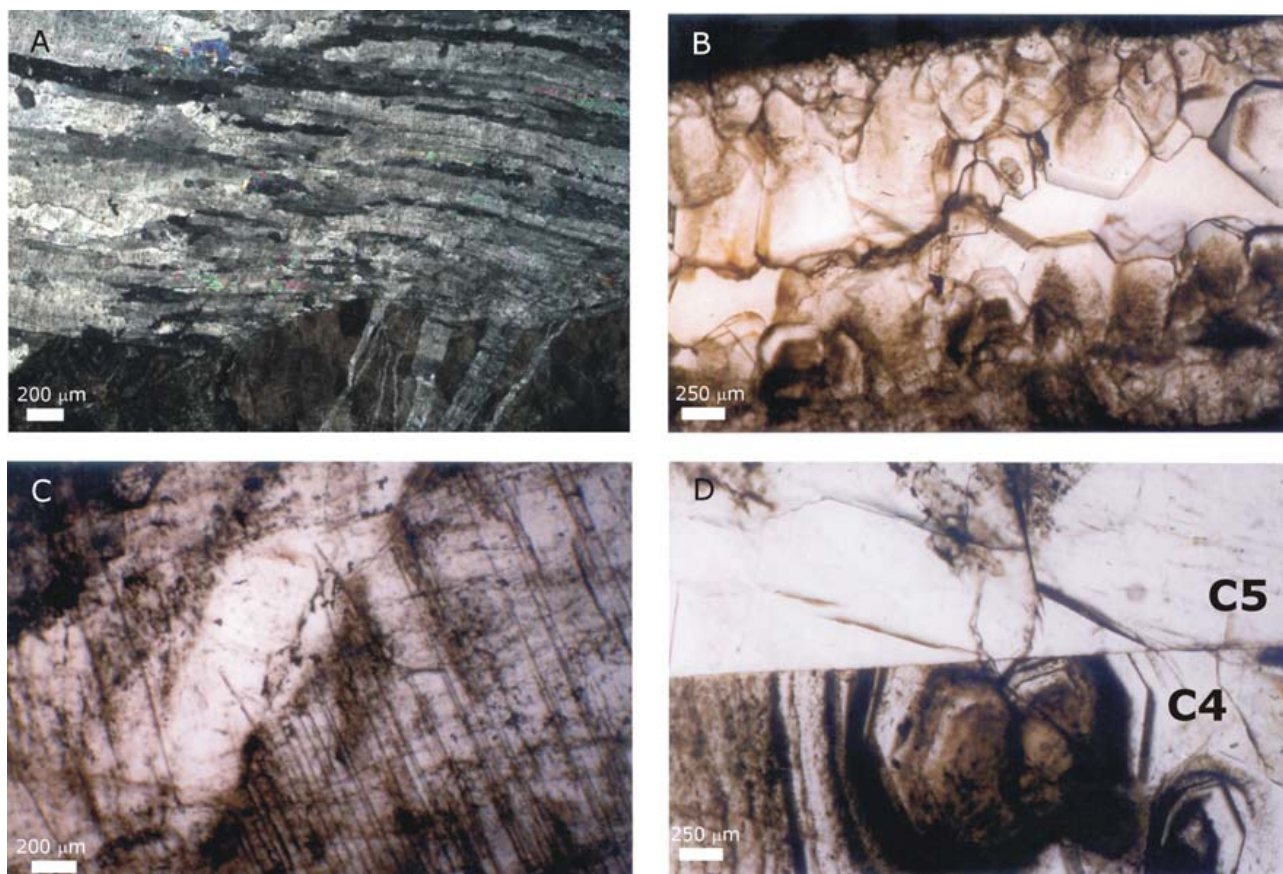


Figure 3. Microphotographs of the Sarıkaya Lineament fault zone, A. Slickenfibers parallel to fault movement, B. Vein parallel with fault movement filled by equant calcites, C. Twinned and transparent calcite crystals of generation C2 in Fig. 4, D. Zone equant calcites of generation C4 that are abruptly cut off before subsequent calcite precipitation of calcite generation C5.

zone, exposed at 1550m, consists of multiple small fault planes with several slickenlines crosscutting the protolith. The overall orientation is 110/70.

4.1 Lineament fault zone

4.1.1 Fabric

The fault zone, comprising the 8 nearly parallel faults and the large normal fault, contains multiple parallel slip planes and zone-parallel layers of fault breccia. The fault rock of all faults is composed of a cohesive limestone breccia or a crush breccia according to Sibson (1977). The limestone in the damage zone is intensely fractured with several small calcite veins and stylolites. Striated slip-planes are present, containing calcite coatings, up to 3 cm thick. The movement on all these faults is dip-slip. The stylolites are preferentially oriented perpendicular to the fault plane and fault movement. The thick coatings display several nearly parallel striated calcite layers and clear slickensteps. The striated fault planes and calcite coatings form the fault core. The calcite coatings on the main fault plane are mainly composed of fibrous calcites, oriented parallel to the fault displacement (Fig. 3A). These fibrous calcites are dull luminescent. Sometimes, they fill veins and show a crack-seal growth with relics of wall rock along the median line. The calcite coatings of the parallel fault zones are mainly built up by equant calcite crystals

(Fig. 3B). Most of the equant calcites in the striated calcite coatings are twinned (Fig. 3C). They show undulous extinction, evidence of recovery and dynamic recrystallisation. The crystals are zoned bright-dull luminescent. The fault core may be composed of several successive generations of calcite coatings (Fig. 4). These coatings crosscut each other and therefore reflect different precipitation phase, each time abruptly cut off by a fault movement before subsequent calcite precipitation (Fig. 3D).

4.1.2 Stable isotope geochemistry

The limestone in the damage zone (fault rock) has an average $\delta^{13}\text{C}$ value of +1.3‰ VPDB and the $\delta^{18}\text{O}$ composition ranges between -0.7 and -3.9‰ V-PDB (Fig. 5). The calcite coatings (C1 to C4 in Fig. 4) and veins filled with fibrous calcites have an average $\delta^{13}\text{C}$ of +1.5‰ and $\delta^{18}\text{O}$ values between -3.0 and -4.0‰ V-PDB. The crystals of the youngest coating (C5 in Fig. 5) have slightly negative $\delta^{13}\text{C}$ values between -0.1 and -0.3‰ V-PDB and a $\delta^{18}\text{O}$ value of -8.8‰ V-PDB. The equant calcite has also a negative $\delta^{18}\text{O}$ value (up to -9.9‰ V-PDB).

The stable isotopic composition of the limestone and veins in the damage zone and most calcite coatings falls within or is close to the range of the protolith. Hence, the carbon and oxygen isotopic composition of the veins and coatings is buffered by the limestones and the protolith is

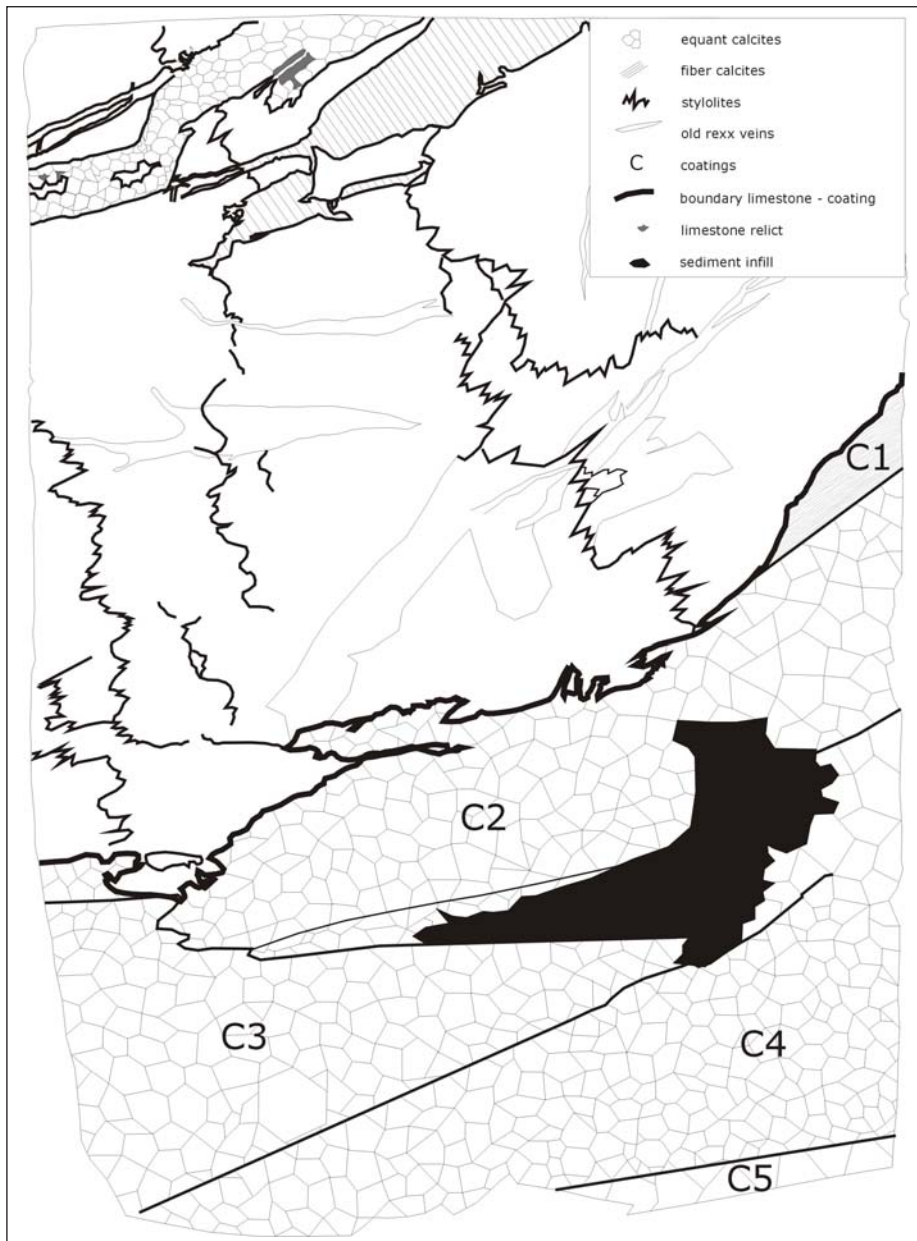


Figure 4. Schematic presentation of the fault rock and calcite coating of a normal fault at Sarıkaya Lineament fault zone. C1 to C5 represent successive calcite generations.

isotopically not reset. The youngest calcite coating and the vein with equant crystals have $\delta^{18}\text{O}$ values much lower than the oxygen isotopic composition of the protolith and also the $\delta^{13}\text{C}$ values of the youngest calcite coating fall outside this range. However, the oxygen isotopic composition of these calcites is within the oxygen isotopic range of meteoric calcite precipitates in the region ($\delta^{18}\text{O} = -9.8$ to -6.5% V-PDB, Verhaert *et al.*, 2004). So, the more negative $\delta^{18}\text{O}$ values possibly reflect an increasing influence of meteoric water in a more open hydrological system.

4.2 Western Summit fault zone

4.2.1 Fabric

The fault rock is intensely brecciated or fractured (Fig. 6). The highly fractured damage zone is composed of non-cohesive breccias, crosscut by several parallel faults (Fig. 7A). This is a typical fault breccia according to the classification of Sibson (1977). Such a non-cohesive

breccia is typical of shallow normal faults crosscutting limestone substrate in the Aegean region (Stewart & Hancock, 1991). It consists of angular limestone fragments, ranging from 2 mm to 2 cm, enveloped by a beige matrix with a volume of 30%. The fault planes are characterised by slickenlines, corrugations, comb fractures and pluck holes. The microscopic fabric analysis of the damage zone demonstrates the occurrence of limestone fragments enveloped in a dark matrix (Fig. 8A). In this dark calcite matrix, small transparent calcite veins and dissolution cavities are filled by transparent equant calcites (Fig. 8B). This breccia can be classified as a particulate cemented mosaic to rubble floatbreccia (cf. Morrow, 1982). A floatbreccia is a descriptive term of a breccia of which the fragments are in general not in contact. The breccia has a polymict composition due to the presence of chert fragments. These cherts are originally present in the Lycian limestone (Muech *et al.*, 2008). In some places, crushed bands developed. The limestone breccia fragments and the dark matrix are dull luminescent. The equant

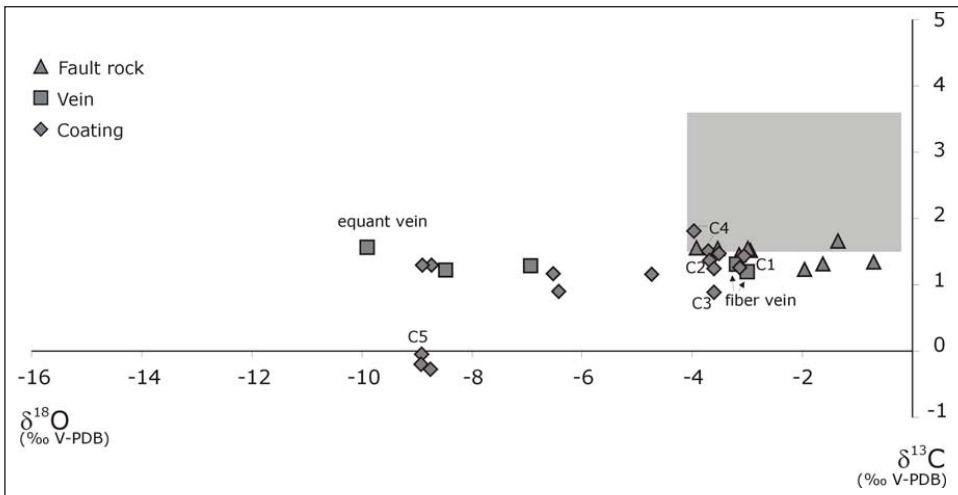


Figure 5. Stable isotope plot of the coating, veins and fault rock from the Sarıkaya Lineament fault zone. Grey box indicates the isotopic signature of the allochthonous Lycian limestone in the area studied (after Muchez *et al.* 2008).

Figure 6. A. Photograph of the Sarıkaya Western Summit fault zone, B. Profile through the Sarıkaya Western Summit fault zone with indication of shatter zone, damage zone and fault core.

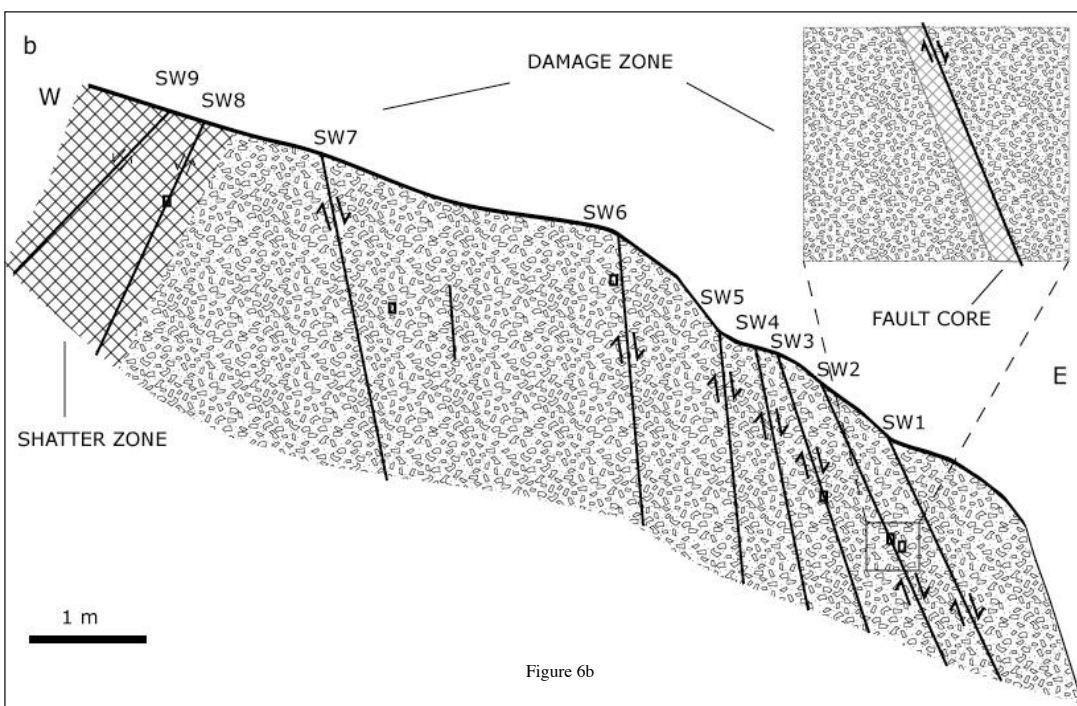


Figure 6b

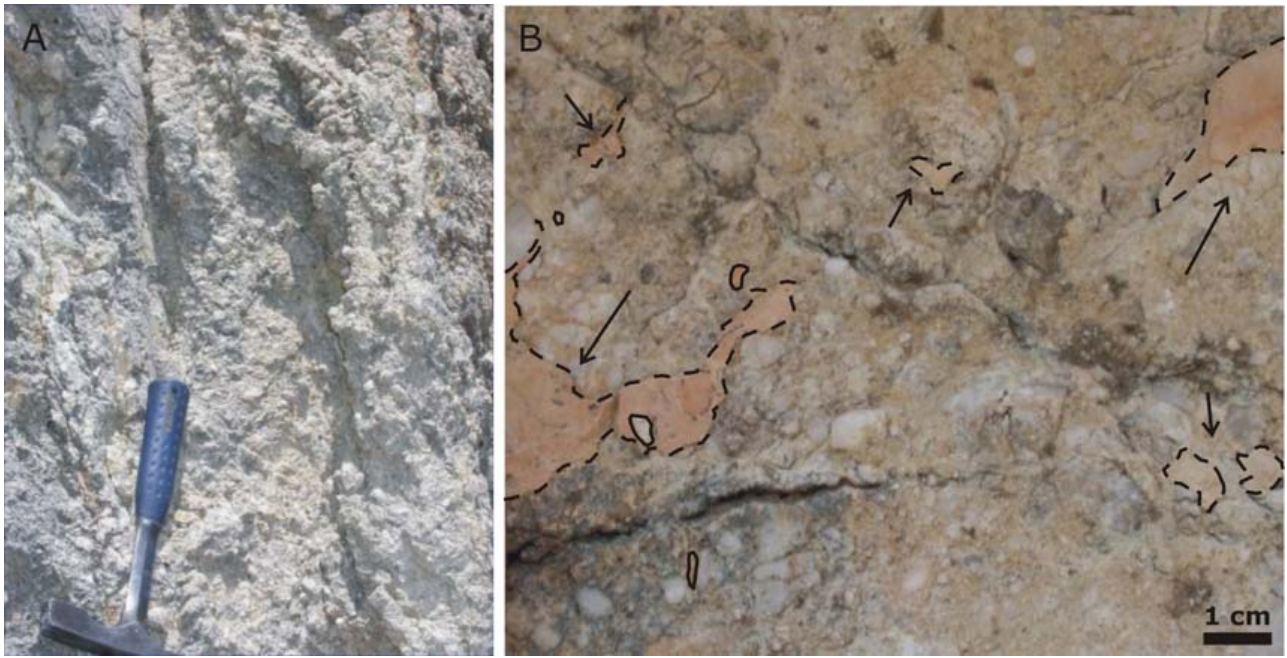


Figure 7. A. Incohesive breccia crosscut by parallel faults (indicated by arrows), B. Detail of a fault plane with relicts of the carapace (indicated by dashed lines and arrows).

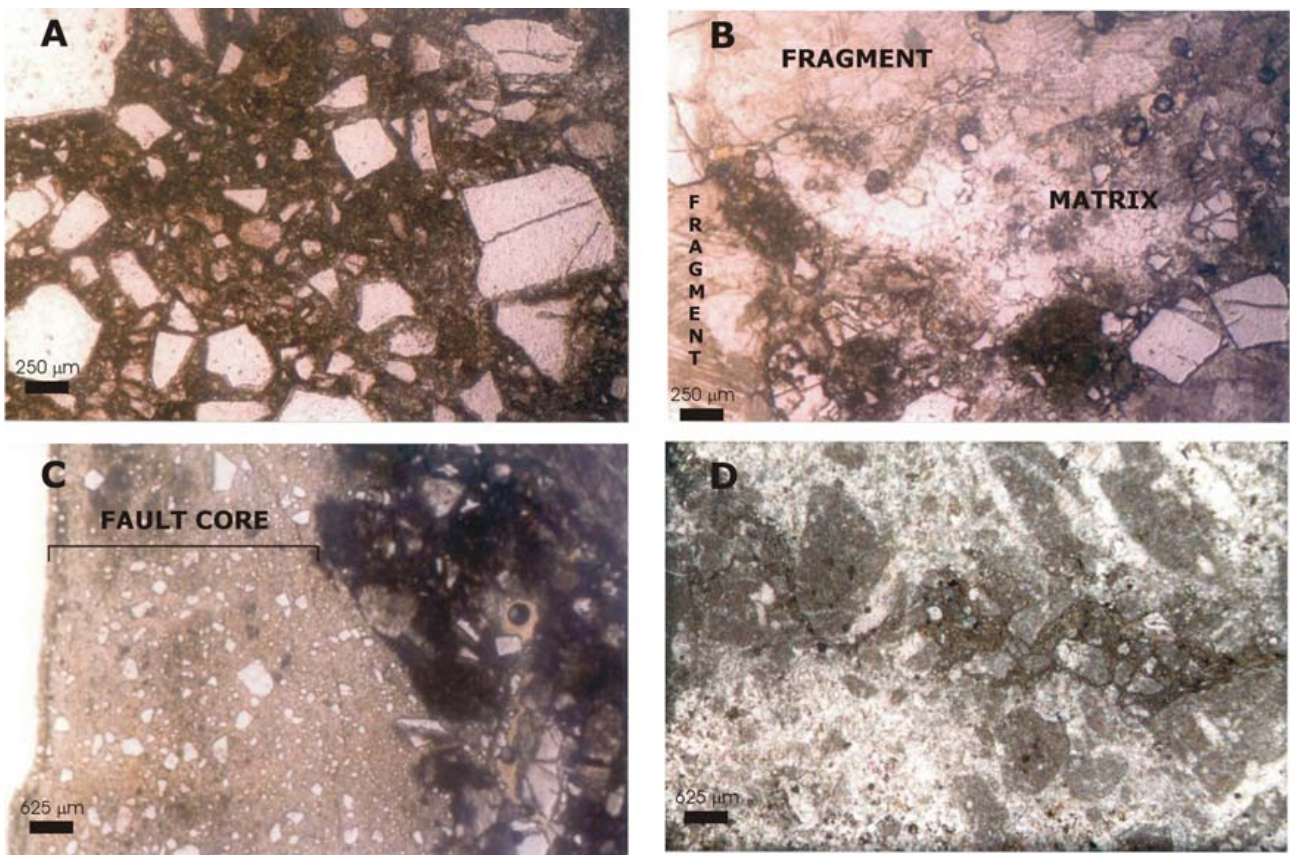


Figure 8. Microphotographs of the Sarikaya Western Summit fault zone. A. Limestone fault breccia in the damage zone characterised by breccia fragments and crushed material in the matrix, B. Limestone fault breccia in the damage zone composed of breccia fragments and a transparent equant calcite cement, C. Crushed fragments in the fault core, D. Fractured limestone in the shatter zone.

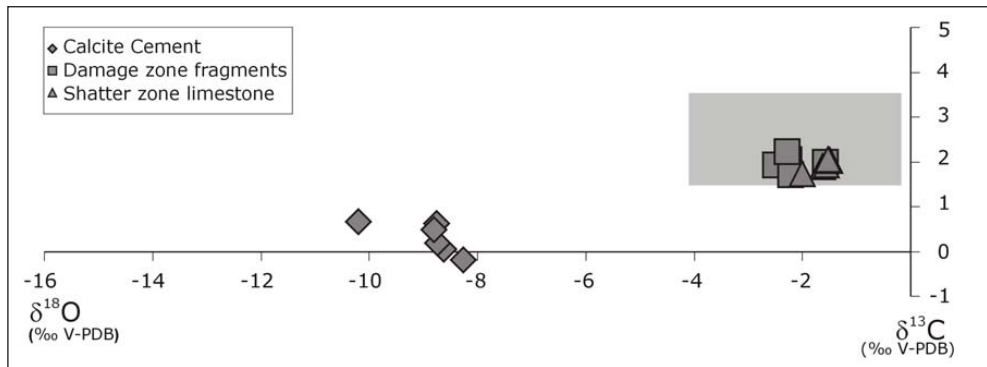


Figure 9. Stable isotope data of the fault zone at Sarıkaya Western Summit. Grey box indicates the stable isotope composition of the Allochthonous Lycian limestone in the area studied (after Mucchez *et al.* 2008).

calcite cement is characterised by a zoned luminescence. The fault core is composed of a cohesive coating of very fine-grained crushed material (Fig. 8C). The resulting breccia is a particulate rubble floatbreccia. This breccia is non-luminescent except some dull luminescent spots, probably of relict limestone fragments.

The fault core, which is still present in one fault, consists of a 1-2 mm thick pink coloured carapace (Fig. 7B) and represents a hard zone (crust).

4.2.2 Stable isotope geochemistry

The limestone in the damage zone (damage zone fragments) shows similar oxygen and carbon isotopic values, which range between -1.5 and -2.5‰ and between

+1.7 and 2.2‰ V-PDB respectively (Fig. 9). The calcite cement in the breccia has lower $\delta^{13}\text{C}$ values between -0.5 and +0.7‰ V-PDB and much lower $\delta^{18}\text{O}$ values between -8.3 and -10.2‰ V-PDB (Fig. 9). The stable isotopic composition of the limestone in the fault zone falls within the range of the protolith. The lower carbon and oxygen isotopic values of the calcite cement fall within the range of meteoric calcite precipitates in the area, however, precipitation from a fluid with a higher oxygen isotopic composition and at higher temperature can not be excluded (Verhaert *et al.*, 2004).

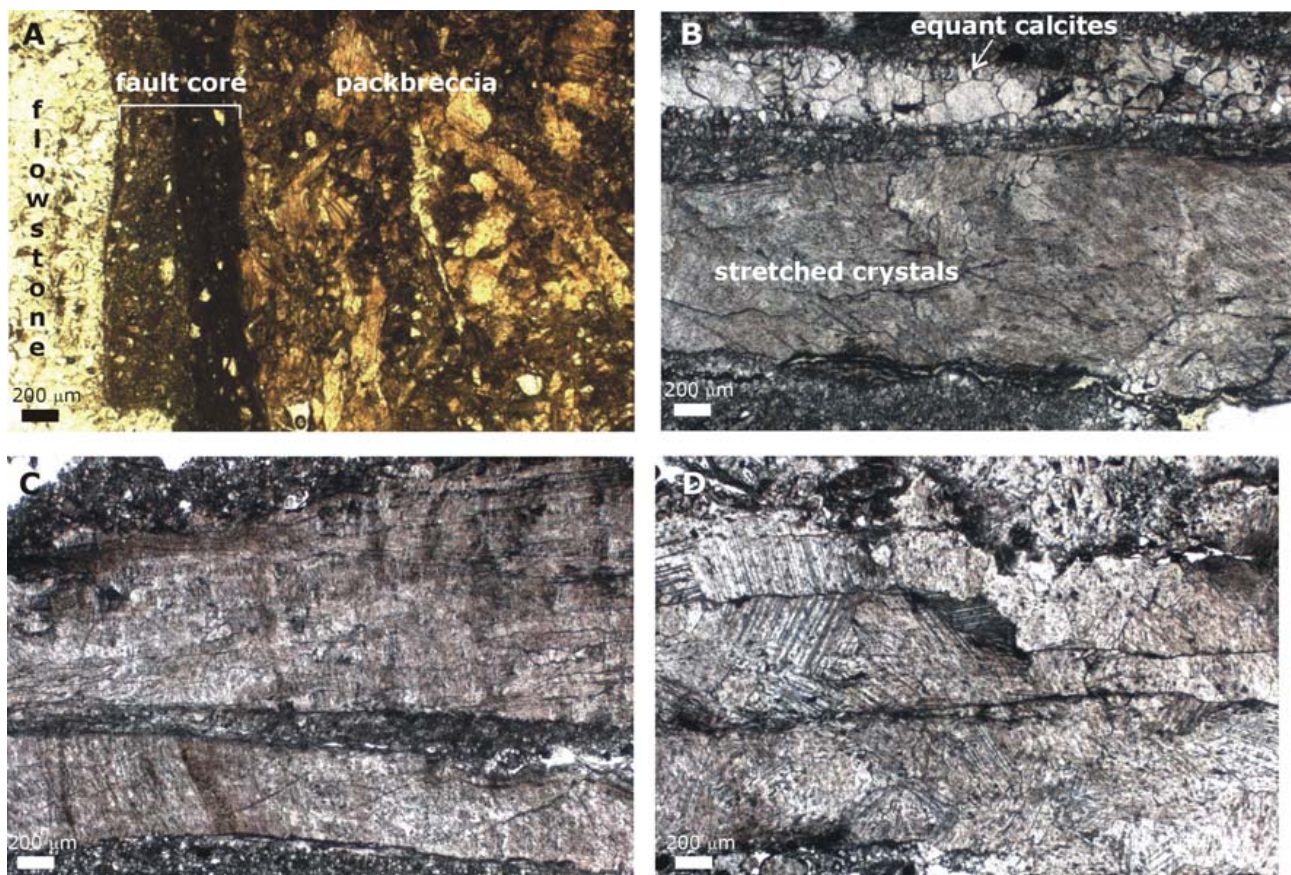


Figure 10. Microphotographs of the Sarıkaya Eastern Summit fault zone, A. Rubble packbreccia with thin fault core and flowstone cover, B. Vein with recrystallized stretched crystals and transparent equant calcites, C. Vein filled with fibrous calcites, D. Relict slickenlines with 3 parallel calcite layers.

4.3 Eastern Summit fault zone

4.3.1 Fabric

The damage zone is composed of a stylobreccia (sensu Stewart & Hancock, 1991) covered with a breccia and flowstone. The microscopic analysis shows a rubble packbreccia (Fig. 10A). This rubble packbreccia is composed of limestone and chert fragments and fragments consisting of equant and blocky calcites with a maximum size of 2 – 3 mm. These calcites are intensely twinned (type II and III of Burkhard, 1993) and show undulous extinction and subgrain development. At several places the twins are fractured and displaced. The contacts between the different fragments are stylolitic. The fault core is composed of a rubble floatbreccia. This fault core floatbreccia is generally built up by the same fragments as the damage zone packbreccia. The matrix consists of very fine crushed material, equant transparent calcites (average size 250 μm) and small recrystallised calcite crystals. The transparent calcites are bright luminescent. Also veins occur in the breccia. These veins are built up by recrystallised stretched calcites (Fig. 10B) and by fibrous crystals (Fig. 10C). These calcites are twinned or show subgrain development. Also relict slickenlines composed of three parallel layers of equant calcite crystals are present (Fig. 10D). The flowstone on top of the fault plane is characterised by columnar crystals (≤ 3.2 mm long). Staining and element analysis reveals an iron-rich nature of the relict slickenlines (3200 ppm) and of the recrystallised small calcite crystals in the matrix of the floatbreccia.

4.3.2 Stable isotope geochemistry

A limestone fragment of the damage zone has a $\delta^{13}\text{C}$ value of +2.4‰ V-PDB and a $\delta^{18}\text{O}$ value of -1.4‰ V-PDB,

within the range of the protolith (Fig. 11). The iron-rich calcites of the slickenlines have $\delta^{13}\text{C}$ values between +1.3‰ and +3.8‰ V-PDB and $\delta^{18}\text{O}$ values between -15.0‰ and -11.1‰ V-PDB. The iron-poor, equant transparent calcite cement of the floatbreccia has a $\delta^{18}\text{O}$ value around -7.3‰ V-PDB and a variable $\delta^{13}\text{C}$ value (up to -7.3‰ V-PDB). The flowstone has a similar $\delta^{18}\text{O}$ value (-7.1‰ V-PDB) and an even lower $\delta^{13}\text{C}$ value (-9.2‰ V-PDB). The $\delta^{18}\text{O}$ values of the iron-rich slickenlines is lower than the $\delta^{18}\text{O}$ composition of the protolith and meteoric calcite precipitates in the region (Verhaert *et al.*, 2004) and reflect precipitation from a fluid at higher temperature. The oxygen isotopic composition of the iron-poor calcites and of the flowstone is within the range of meteoric calcites and the negative $\delta^{13}\text{C}$ values is most likely due to the influence of soil-gas CO_2 (cf. Salomons *et al.*, 1978; Muchez *et al.*, 1993). The fluid responsible for their precipitation is a near-surface meteoric fluid.

4.4 Quarry fault zone

4.4.1 Fabric

A cross-section through the coatings and fault rock, which can be classified as a stylobreccia, reveals the presence of corrugations. The microscopic analysis of the rocks in the damage zone shows that the cohesive fault rock limestone is intensely fractured with calcite veins up to 0.6 mm wide, resulting in a cemented crackle packbreccia (Morrow, 1982). Random oriented stylolites are present. The fault core contains thin, striated calcite coatings. The coatings are maximum 1 cm thick. The calcite coatings are composed of two calcite generations. The first generation consists of twinned, equant and blocky calcite crystals (≥ 2 mm). These calcite crystals contain dark tiny

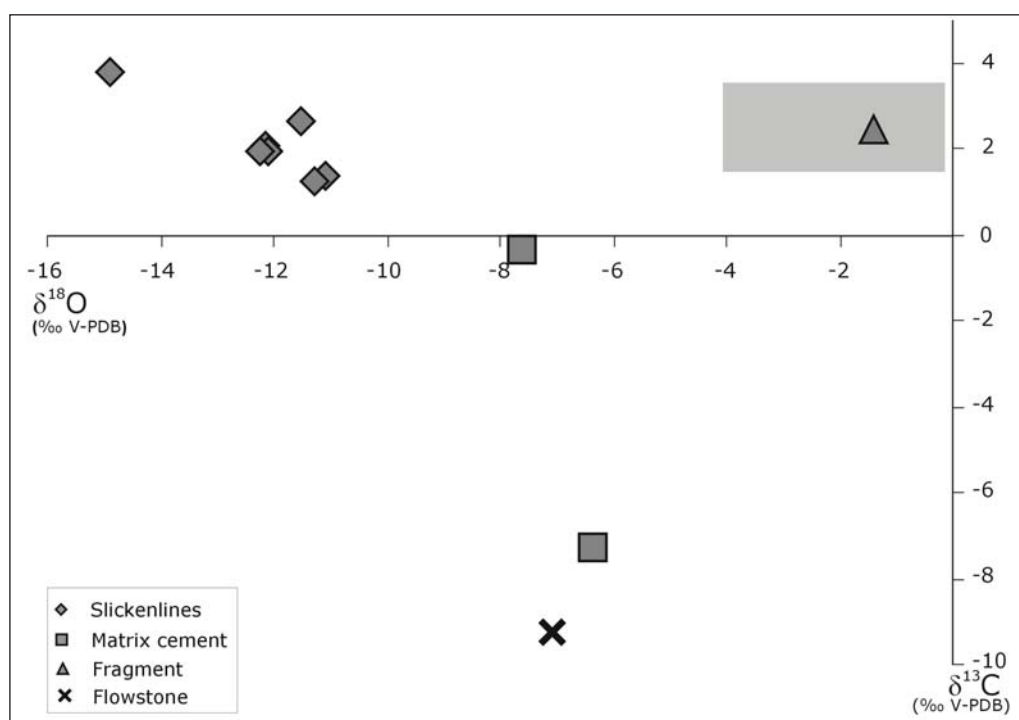


Figure 11. Stable isotope data of the fault zone at Sarıkaya Eastern Summit. Grey box indicates the stable isotope composition of the allochthonous Lycian limestone in the area studied (after Muchez *et al.* 2008).

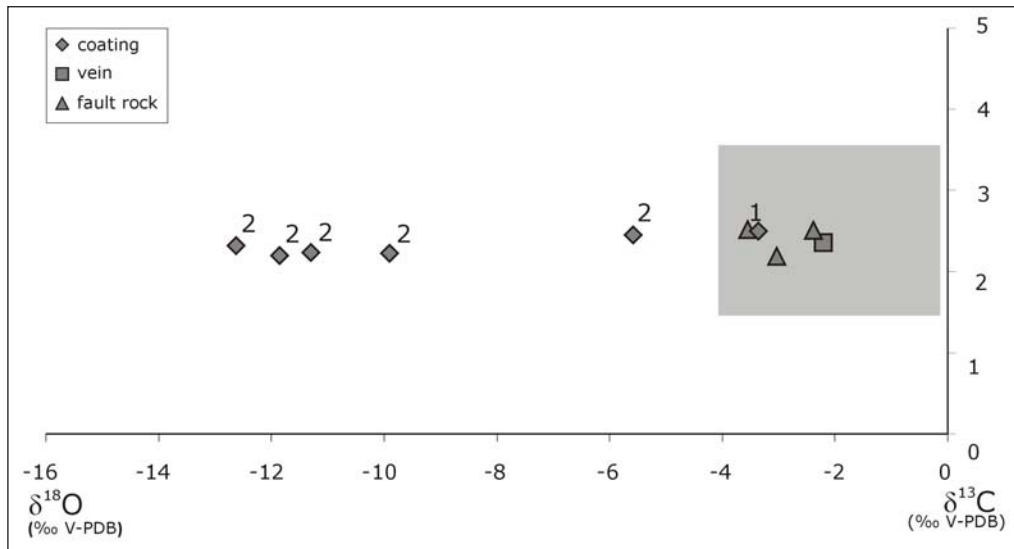


Figure 12. Stable isotope data of the fault zone at Sankaya Quarry. The numbers 1 and 2 represent the samples from the first and the second calcite coating respectively. Grey box indicates the stable isotope composition of the allochthonous Lycian limestone in the area studied (after Muchez *et al.* 2008).

inclusions ($\leq 3 \mu\text{m}$). Transparent, equant and blocky calcites ($\leq 600 \mu\text{m}$) form the second generation.

Staining and elemental analyses of the calcite coating show a high iron content (1000 ppm).

4.4.2 Stable isotope geochemistry

The fault rock, a vein in the fault core and the first generation of calcite coating have $\delta^{13}\text{C}$ values between +2.2 and +2.5‰ V-PDB and $\delta^{18}\text{O}$ values between -2.2 and -3.4‰ V-PDB, within the range of the protolith (grey box of Fig. 12). The $\delta^{13}\text{C}$ values of the second generation of calcite coating are around +2.3‰ V-PDB, however, the $\delta^{18}\text{O}$ values show a broad range between -12.6 and -5.6‰ V-PDB. The similar isotopic composition of the vein and first generation of calcite coating as the protolith indicate an isotopic buffering of the ambient fluid. Also the similarity in carbon isotopic values between the second generation of calcite coating and host-rock implies a carbon buffering. However, the $\delta^{18}\text{O}$ values show a wide range, which is even lower than that of meteoric calcite precipitates in the region. The latter reflects the influence of higher precipitation temperature.

5. Fault zone architecture

The fault zones studied can be subdivided in three groups, each representing a particular structural level. The first group is represented by the two fault zones at the lowest elevation, the LFZ and the QFZ (~1500 – 1550 m). The damage zone is composed of a cemented crackle packbreccia. Several calcite veins and stylolites are present in these stylobreccia. Multiple parallel striated calcite coatings are present on the fault plane. Progressive deformation at the LFZ is responsible for the multiple parallel slip planes. These fault zones do not contain well-developed incohesive breccia belts, or a zone of floatbreccias or rubble packbreccias. The protolith is in direct contact with the stylobreccia. The fault core is composed of striated calcite coatings. According to Stewart & Hancock (1990), the presence or absence of

stylobreccia within a fault zone is related to whether or not there is a salient block of uneroded bedrock cover remaining in the hanging wall at the time the free surface was displaced. It is suggested that such hanging wall salients inhibit the tendency of slip planes to propagate into the more brecciated hanging wall and, instead, concentrate deformation along the main fault plane, thereby creating meter-wide stylobreccia zones. This first group can be classified as a “localised conduit” (Caine *et al.*, 1996).

A second group can be described as a “combined conduit-barrier”. The faults at ESFZ, at the intermediate elevation (1650m) form part of this group. The fault rock is characterised by multiple brecciation phases resulting in a carapace at the fault plane contact. The fault zone is composed of a rubble packbreccia with on top a carapace of rubble floatbreccia. The floatbreccia contains besides limestone and chert fragments also relicts of slickenlines. The packbreccia could be originally part of the first group of fault rocks. A more profound brecciation, however, caused the formation of the carapace. The fault core of the second group is composed of a fault-parallel carapace. This carapace is characterised by a breccia with a higher matrix/fragment ratio (i.e. floatbreccia). An ongoing brecciation causes a more profound crushing of the fragments and a higher matrix/fragment ratio.

The third group consists of the fault at the highest elevation (~1700m), forming part of the WSFZ. The fault zone is composed of a very wide damage zone of incohesive breccia and only a small fault core. It represents a “distributed conduit” (Caine *et al.*, 1996). The fault zone may indicate multiple episodes of slip and overprinting of successive deformation events. Fault displacement, which is an indicator of the amount of strain accumulated within a fault zone, is according to Micarelli *et al.* (2003) related to the damage zone width. In general, at outcrop scale (Shipton & Cowie, 2001) and micro-scale (Vermilye & Scholtz, 1998), the fault zone becomes larger with increasing displacement (e.g. Cello, 2000). Following Vita-Finzi & King (1985) and Petit & Barquins (1988),

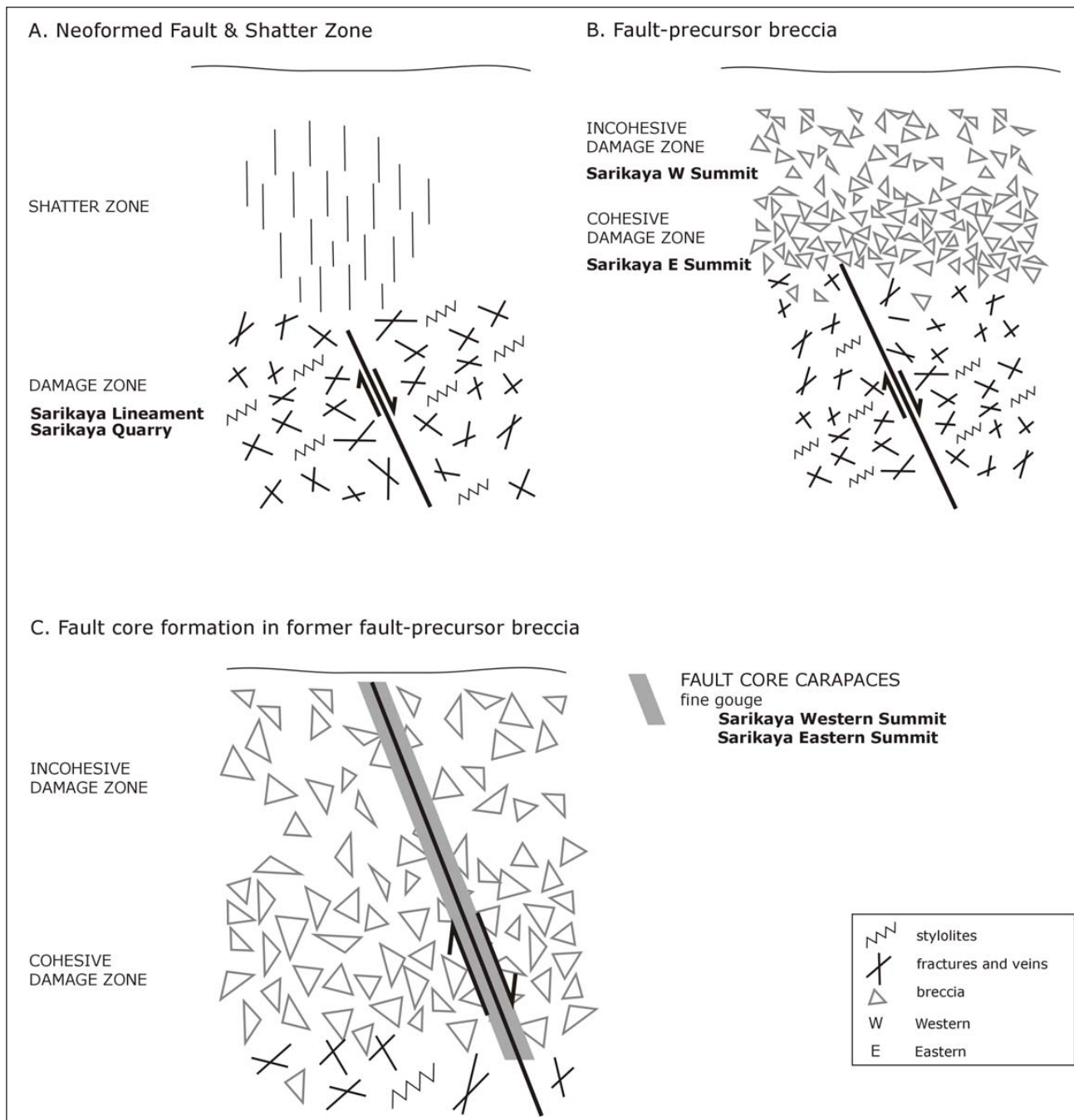


Figure 13. Different stages of normal fault development as deduced from the fabric analysis of the studied faults. A. Neoformed fault and shatter zone, B. Fault-precursor breccia, C. Fault core formation in former fault-precursor breccia.

these broad belts of brecciated and shattered rocks can be interpreted as products of distributed deformation above and ahead of upwards-propagating tip lines of normal faults. According to Hancock & Barka (1987) such belts of fault-precursor deformation are likely to be developed in hanging walls, which preferentially experience dilational deformation. The wide damage zone breccia can be interpreted as a fault-precursor breccia of upwards-propagating slip-planes. Later through-going slip-planes result in the formation of fault cores.

The LFZ and the fault planes in the WSFZ are both composed of multiple slip-planes crosscutting cohesive stylobreccias and incohesive breccias respectively. The

wide damage zone of the WSFZ is interpreted as a precursor breccia of upwards-propagating slip planes. Compared with the damage zone of the WSFZ, the LFZ reflects the kinematic expression of these through-going normal faults, but at greater depth. The QFZ is characterised by a stylobreccia damage zone and a striated calcite coating on top, forming the core of the zone. The ESFZ has also a damage zone composed of stylobreccia fault rocks. The fault core, however, is a floatbreccia with relict slickenlines. These fault zones also reflect a different stage in the development of a normal fault zone.

6. Normal fault zone development

The contrasting styles of fault zone architecture allow obtaining a good insight in the development and evolution of a normal fault zone (Fig. 13A). The earliest stage of normal fault development occurs with the upward propagation of a neoformed fault. The normal fault cuts carbonate protolith and deformation along the fault plane creates fractures and tectonic stylolites (LFZ and QFZ). This propagation is accompanied by the formation of a fault-precursor damage zone ahead of the fault tip. Later motion on the fault as it propagates towards the free surface leads to additional deformation in the immediate vicinity of the fault tip. This motion brecciated the already fractured bedrocks, giving rise to a fault-precursor breccia (Fig. 13B). This breccia is composed of closely spaced and randomly oriented fractures and ultimately an incohesive breccia belt is created. At the fault tip, deformation is accommodated by intense localized fragmentation and brecciation of the adjacent shatter zone. Evidence for this stage is found in the damage zone, cohesive fault-precursor breccias at ESFZ.

Once slip planes reach the free surface by propagating through its own (in)cohesive breccia belt, co-seismic deformation is restricted to a relatively narrow zone of attrition and/or mineralisation adjacent to the slip plane (Fig. 13C). The through-going slip planes result in the formation of fault cores. Hence, later propagation of a fault plane through its fault precursor breccia results in the deformation being concentrated along the fault plane and the reconstitution of the fault precursor breccia into a fine gouge or attrition breccia, thus forming compact breccia sheets. Evidence for this stage can be found in the carapaces at WSFZ and ESFZ. On emergence on the surface, the fault core forms an indurated carapace (compact breccia sheet) to the fault plane that protects the underlying fault precursor breccia from denudation.

7. Fault related fluid flow

7.1 Localised conduit

The stylobreccia of the LFZ and the QFZ has a low permeability. These fault zones contain, however, multiple, striated calcite coatings. So, although the fault core material has low matrix permeability, they did not always act as a barrier to flow. During fault movement, permeability is greatly enhanced at the fault plane. This results in a localized conduit. The permeability difference with the low permeable stylobreccia ($K_D < K_F$ during fault movement) creates a co-seismic, focused fluid flow parallel with the fault plane.

The isotopic composition of most calcite precipitates ($\delta^{13}\text{C}$ values between +0.8 and +2.5‰ V-PDB and $\delta^{18}\text{O}$ values between -4 and -2.2‰ V-PDB) along the fault plane are buffered by the protolith. In such a setting, the calcium carbonate of the precipitates could have originated from pressure solution (Fig. 4) of the limestone host rock (cfr Muchez *et al.* 1995). The isotopic composition of the

youngest calcite generation (with negative $\delta^{13}\text{C}$ values between -0.3 and -0.1‰ V-PDB and $\delta^{18}\text{O}$ values between -5.6 and -12.6‰ V-PDB) in the fault zone, however, reflects an open fluid flow system with fluids originating from greater depth (e.g. at QFZ). The calcite coatings on the fault planes are pre- and post-dated by fault movement. This reinforces the interpretation that episodes of fluid flow and hydrothermal precipitation are intimately related to repetitive increments of seismic slip. In this case, the fault systems cannot be regarded as a passive fluid conduit and fluid migration is dynamically related with faulting.

7.2 Combined conduit-barrier

Due to the cohesive nature of the damage zone fault rock and the fault core carapace, their permeability is quasi similar ($K_D \approx K_F$). This results in a combined conduit-barrier system and a more dispersed co-seismic and inter-seismic fluid flow. The stable isotopic composition of the calcite cement in the floatbreccia (variable $\delta^{13}\text{C}$ values up to -7.3‰ V-PDB and $\delta^{18}\text{O} \approx -7$ ‰ V-PDB) is not buffered by the host-rock and indicates precipitation from a meteoric fluid at near-surface temperatures. The iron-rich calcites of the slickenlines on the fault planes formed from a fluid at higher temperatures and originating from the deeper subsurface.

7.3 Distributed conduit

The WSFZ may reflect distributed strain (e.g. Caine *et al.*, 1996). The damage zone is characterised by a very high permeability ($K_D > K_F$), resulting in a distributed conduit (Caine *et al.*, 1996). The presence of the higher permeable damage zone causes the fault zone to act as a conduit for flow. The small amount of calcite cement present in the breccia ($\delta^{13}\text{C}$ values between -0.5 and +0.7‰ V-PDB and $\delta^{18}\text{O}$ between -8.3 and -10.2‰ V-PDB) is not buffered by the host-rock and possibly precipitated from meteoric water at near surface temperatures. Static fault related fluid flow could have been responsible for calcite cementation of the breccia.

8. Conclusions

The earliest stage of normal fault zone development occurs with the upward propagation of a neoformed fault. Seismic deformation is responsible for the development of a low permeable stylobreccia at depth. During fault movement, permeability is greatly enhanced at the fault plane contact. This permeability enhancement causes a fluid-pressure differential responsible for co-seismic, focused fluid flow parallel with the fault plane. Calcites on the fault plane and in veins in the damage zone precipitated from rock buffered fluids. Calcite precipitation destroys permeability. During repetitive increments of seismic slip, permeability is renewed at the fault plane contact and fluids are expelled. These increments of seismic slip lead to fault propagation. This fault propagation is accompanied by the formation of a fault precursor breccia ahead of the fault tip by intense localized

fragmentation and brecciation of the adjacent shatter zone. This leads to a cohesive breccia where confining pressure is still high and an incohesive breccia near the surface. The cohesive damage zone acts as a combined conduit-barrier system and a more dispersed, co-seismic fluid flow is present near the fault plane contact. The near-surface, incohesive damage zone is characterised by a high permeability, which leads to a dispersed fluid flow. Meteoric water can easily infiltrate which leads to static fluid interaction with the normal fault.

Later propagation of a fault plane through its fault-precursor breccia belt results in the deformation concentrated along the fault plane and the evolution of the fault-precursor into a fine gouge or attrition breccia. Once a slip plane reaches the free surface by propagating through its own (in)cohesive breccia belt, co-seismic deformation is restricted to a relatively narrow zone of attrition. In the case of the cohesive damage zone, fluid flow is enhanced adjacent to the slip plane. The fault related fluid is in equilibrium.

9. Acknowledgements

We are grateful to V. Hallet and S. Vandycke for their constructive reviews of this manuscript and to J.-Cl Duchesne for the editorial handling. We would like to thank Herman Nijs for the careful preparation of the numerous thin sections. The PhD research of Griet Verhaert was financed by the Institute for the Promotion of Innovation through Science and Technology in Flanders (IWT- Vlaanderen). This research was also supported by a Concerted Action of the Flemish Government (GOA 02/9) and Marc Waelkens is thanked for his continuous support. M. Sintubin is Research Associate of the Onderzoeksfonds K.U.Leuven.

10. References

- ANDERSON, R.N., FLEMINGS, P., LOSH, S. & AUSTIN, J., 1994. Gulf of Mexico growth fault drilled, seen as oil, gas migration pathway. *Oil and Gas Journal*, 94: 97-104.
- ANTONELLI, M. & AYDIN, A., 1994. Effect of faulting on fluid flow in porous sandstones: petrophysical properties. *American Association of Petroleum Geologists Bulletin*, 78: 355-377.
- BARKA, A.A., REILINGER, R., SAROGLU, F. & SENGÖR, A.M.C., 1995. The Isparta Angle: Its importance in the neotectonics of the Eastern Mediterranean Region. In: *International Earth Sciences Colloquium on the Aegean Region* 1: 3-17.
- BILLI, A., SALVINI, F. & STORTI, F., 2003. The damage zone-fault core transition in carbonate rocks: implications for fault growth, structure and permeability. *Journal of Structural Geology*, 25: 1779-1794.
- BOZKURT, E., 2001. Neotectonics of Turkey – a synthesis. *Geodynamica Acta*, 14: 3-30.
- BREESCH, L., SWENNEN, R. & VINCENT, B., in press. Fluid flow reconstruction in hanging and footwall carbonates: Compartmentalization by Cenozoic reverse faulting in the Northern Oman Mountains (UAE). *Marine and Petroleum Geology*, doi:10.1016/j.marpetgeo.2007.10.004.
- BURKHARD, M., 1993. Calcite twins, their geometry, appearance and significance as stress-strain markers and indicators of tectonic regime: a review. *Journal of Structural Geology*, 15: 351-368.
- CAINE, J.S., EVANS, J.P. & FORSTER, C.B., 1996. Fault zone architecture and permeability structure. *Geology*, 24: 1025-1028.
- CELLO, G., 2000. The resolution of geological analysis and models for earthquake faulting – Preface. *Journal of Geodynamics*, 29: 149
- COPLEN, T.B., KENDALL, C. & HOPPLE, J., 1983. Comparison of stable isotope reference samples. *Nature*, 302: 236-238.
- COX, S.F., KNACKSTEDT, M.A. & BRAUN, J., 2001. Principles of structural controls on permeability and fluid flow in hydrothermal Systems. *Reviews in Economic Geology*, 14: 1-24
- DEGRYSE, P., MUCHEZ, PH., LOOTS, L., VANDEPUT, L. & WAELEKENS, M., 2003. The building stones of Roman Sagalassos (SW Turkey): facies analysis and provenance. *Facies*, 48: 9-22.
- DEGRYSE, P., MUCHEZ, PH., TROGH, E. & WAELEKENS, M., 2008. The natural building stones of Hellenistic to Byzantine Sagalassos: provenance determination through stable isotope geochemistry. In: *Proceedings of the Seventh International Conference of ASMOSIA*, Thassos, Greece, 2003.
- ETHERIDGE, M.A., WALL, V.J. & COX, S.F., 1984. High fluid pressures during regional metamorphism and deformation: Implications for mass-transport and deformation mechanisms. *Journal of Geophysical Research*, 89: 4344-4358.
- EVANS, J., FORSTER, C. & GODDARD, J., 1997. Permeability of fault-related rocks and implications for hydraulic structure of fault zones. *Journal of Structural Geology*, 19: 1393-1404.
- FRISIA-BRUNI, S., JADOUL, F. & WEISSERT, H., 1989. Evinosponges in the Triassic Esino Limestone (Southern Alps): documentation of early lithification and late diagenetic overprint. *Sedimentology*, 36: 685-699.
- GIBSON, R.G., 1994. Fault-zone seals in siliciclastic strata of the Columbus Basin, offshore Trinidad. *American Association of Petroleum Geologists Bulletin*, 78: 1327-1385.
- HANCOCK, P.L. & BARKA, A.A., 1987. Kinematic indicators on active normal faults in western Turkey. *Journal of Structural Geology*, 9: 573-584.
- HULIN, C.D., 1929. Structural control of ore deposition. *Economic Geology*, 24: 15-49.

- KNIFE, R.J., 1993. The influence of fault zone processes and diagenesis on fluid flow. *In: Horbury, A.D., Robinson, A.G. (eds) Diagenesis and basin development*. American Association of Petroleum Geologists Studies, 36: 135-151.
- MICARELLI, L., BENEDICTO, A. & WIBBERLEY, C.A., 2006. Structural evolution and permeability of normal fault zones in highly porous carbonate rocks. *Journal of Structural Geology*, 28: 1214-1227.
- MICARELLI, L., MORETTI, I. & DANIEL, J.M., 2003. Structural properties of rift-related normal faults: the case study of the Gulf of Corinth, Greece. *Journal of Geodynamics*, 36: 275-303.
- MORROW, D.W., 1982. Descriptive field classification of sedimentary and diagenetic breccia fabrics in carbonate rocks. *Bulletin of Canadian Petroleum Geology*, 30: 227-229.
- MUCHEZ, PH., PEETERS, C., KEPPENS, E. & VIAENE, W.A., 1993. Stable isotopic composition of paleosols in the Lower Visean of Eastern Belgium – Evidence of evaporation and soil-gas CO₂. *Chemical Geology*, 106: 389-396.
- MUCHEZ, PH., SLOBODNIK, M., VIAENE, W.A. & KEPPENS, E., 1995. Geochemical constraints on the origin and migration of palaeofluids at the northern margin of the Variscan foreland, southern Belgium. *Sedimentary Geology*, 96: 191-200.
- MUCHEZ, PH., HEIJLEN, W., BANKS, D., BLUNDELL, D., BONI, M. & GRANDIA, F., 2005. Extensional tectonics and the timing and formation of basin-hosted deposits in Europe. *Ore Geology Reviews*, 27: 241-267.
- MUCHEZ, PH., LENS, S., DEGRYSE, P., CALLEBAUT, K., DEDEREN, M., HERTOGEN, J., JOACHIMSKI, M., KEPPENS, E., OTTENBURGS, R., SCHROYEN, K. & WAEKENS, M., 2008. Petrography, mineralogy and geochemistry of the rocks in the area of the archaeological site of Sagalassos, SW Turkey. *In: Degryse, P., Waelkens, M. (eds) Sagalassos 6. Geo- and Bio-Archaeology in the territory of Sagalassos*, University Press Leuven, Leuven.
- NEWHOUSE, W.H., 1942. *Ore deposits as related to structural features*. Princeton University Press, Princeton.
- PETIT, J.P. & BARQUINS, M., 1988. Can natural faults propagate under mode II conditions? *Tectonics*, 7: 1243-1256.
- PITTMAN, E.D., 1981. Effect of fault-related granulation on porosity and permeability of quartz sandstones, Simpson group (Ordovician), Oklahoma. *Bulletin of the American Association of Petroleum Geologists*, 63: 2381-2387.
- POISSON, A., ORSAY, A., AKAY, E., DUMONT, J.F. & UYSAL, S., 1984. The Isparta Angle : a Mesozoic palaeorift in the Western Taurides. *In: Tekeli, O., Gönçüoğlu, M.C. (eds) Proceedings of the International Symposium on the Geology of the Taurus Belt*. Mineral research and exploration institute (MTA), Ankara: 11-26.
- ROBERTS, S.J., 1995. Episodic expulsion of abnormally pressured fluid along growth faults. *Geological Society of America Abstracts*, 27: 329.
- ROSALES, I., QUESADA, S. & ROBLES, S., 2001. Primary and diagenetic isotopic signals in fossils and hemipelagic carbonates: the Lower Jurassic of northern Spain. *Sedimentology*, 48: 1149-1169.
- SALOMONS, W., GOUDIE, A. & MOOK, W.G., 1978. Isotopic composition of calcrete deposits from Europe, Africa and India. *Earth Surface Processes*, 3: 43-57.
- ŞENEL, M., 1997. *Türkiye Jeoloji Haritaları, Isparta Paftası (Geological maps of Turkey at 1:250000 scale, Isparta sheet)*. Mineral Research and Exploration Institute of Turkey (MTA), Ankara.
- ŞENGOR, A.M.C., GÖRÜR, N. & ŞAROĞLU, O., 1985. Strike-slip faulting and related basin formation in zones of tectonic escape: Turkey as a case study. *In: Biddle, K.T., Christie-Blick, N. (eds) Strike-slip deformation, basin formation and sedimentation*. Society of Economic Palaeontologists and Mineralogists Special Publication, 37: 227-264.
- SHIPTON, Z.K. & COWIE, P.A., 2001. Damage zone and slip-surface evolution over micrometer to kilometer scales in high-porosity Navajo sandstone, Utah. *Journal of Structural Geology*, 23: 1825-1844.
- SIBSON, R.H., 1977. Fault rocks and fault mechanisms. *Journal of the Geological Society of London*, 133: 191-231.
- SIBSON, R.H., 2000. Fluid involvement in normal faulting. *Journal of Geodynamics*, 29: 469-499.
- SIBSON, R.H., ROBERT, F. & POULSEN, H., 1988. High-angle reverse faults, fluid-pressure cycling and mesothermal gold-quartz deposits. *Geology*, 16: 551-555.
- SIMILOX-TOHON, D., 2006. *An integrated geological and archaeoseismological approach of the seismicity in the territory of Sagalassos (SW Turkey). Towards the identification of active faults in the Burdur-Isparta region*. Unpublished Ph.D. thesis, Katholieke Universiteit Leuven, 322pp.
- SIMILOX-TOHON, D., SINTUBIN, M., MUCHEZ, P., VANHAVERBEKE, H., VERHAERT, G. & WAEKENS, M., 2005. Identification of a historical morphogenic earthquake through trenching at ancient Sagalassos (SW Turkey). *Journal of Geodynamics*, 40: 279-293.
- SIMILOX-TOHON, D., SINTUBIN, M., MUCHEZ, PH., VERHAERT, G., VANNESTE, K., FERNANDEZ-ALONSO, M., VANDYCKE, S., VANHAVERBEKE, H. & WAEKENS, M., 2006. The identification of an active fault by a multidisciplinary study at the archaeological site of Sagalassos (SW Turkey). *Tectonophysics*, 420: 371-387.
- SIMILOX-TOHON, D., FERNANDEZ-ALONSO, M., VANNESTE, K., MUCHEZ, PH. & SINTUBIN, M., 2008. An integrated neotectonic study of the Çanaklı basin (SW Turkey): remote sensing, surface geology and near-surface geophysics. *In: Degryse, P., Waelkens, M. (eds) Sagalassos 6. Geo- and Bio-Archaeology in the territory of Sagalassos*, University Press Leuven, Leuven.

- SINTUBIN, M., MUCHEZ, PH., SIMILOX-TOHON, D., VERHAERT, G., PAULISSEN, E. & WAEKENS, M., 2003. Seismic catastrophes at the ancient city of Sagalassos (SW Turkey) and their implications for the seismotectonics in the Burdur-Isparta area. *Geological Journal*, 38: 359-374.
- SMITH, B.N., 1980. Citation classis – Two categories of C-13/C-12 ratios for higher plants. *Agriculture biology and environmental sciences*, 43: 10-19.
- SMITH, L., FORSTER, C.B. & EVANS, J.P., 1990. Interaction of fault zones, fluid flow and heat transfer at the basin scale. In: *Hydrogeology of permeability environments*. International Association of Hydrogeologists, 2: 41-67.
- STEWART, I.S., & HANCOCK, P.L., 1990. Brecciation and fracturing within neotectonic normal fault zones in the Aegean region. In: KNIPE, R.J., RUTTER, E.H. (eds) *Deformation mechanisms, rheology and tectonics*. Geological Society Special Publications, 54: 105-112.
- STEWART, I.S. & HANCOCK, P.L., 1991. Scales of structural heterogeneity within neotectonic normal fault zones in the Aegean region. *Journal of Structural Geology*, 13: 191-204.
- TELLAM, J.H., 1995. Hydrochemistry of the saline groundwaters of the Lower Mersey Basin Permo-Triassic sandstone aquifer, UK. *Journal of Hydrology*, 165: 45-84.
- TEN VEEN, J.H., 2004. Extension of Hellenic forearc shear zones in SW Turkey: the Pliocene-Quaternary deformation of the Esen Cay Basin. *Journal of Geodynamics*, 37: 181-204.
- VERHAERT, G., MUCHEZ, PH., SINTUBIN, M., SIMILOX-TOHON, D., VANDYCKE, S., KEPPENS, E., HODGE, E.J. & RICHARDS, D.A., 2004. Origin of palaeofluids in a normal fault setting in the Aegean region. *Geofluids*, 4: 300-314.
- VERHAERT, G., SIMILOX-TOHON, D., VANDYCKE, S., SINTUBIN, M. & MUCHEZ, PH., 2006. Different stress states in the Burdur-Isparta region (SW Turkey) since Late Miocene times: a reflection of a transient stress regime. *Journal of Structural Geology*, 28: 1067-1083.
- VERMILYE, J.M. & SCHOLTZ, C.H., 1998. The process zone: a microstructural view of fault growth? *Journal of Geophysical Research*, 103: 12223-12237.
- VERSTRAETEN, G., PAULISSEN, E., LIBRECHT, I. & WAEKENS, M., 2000. Limestone platforms around Sagalassos resulting from giant mass movements. In: Waelkens, M., Loots, L. (eds) *Sagalassos V, Report on the survey and excavation campaigns of 1996 and 1997*. Acta Archaeologica Lovaniensia 11B, Leuven University Press, Leuven: 451-461.
- VITA-FINZI, C. & KING, G.C.P., 1985. The seismicity, geomorphology and structural evolution of the Corinth area of Greece. *Philosophical Transactions of the Royal Society*, A314: 379-407.